Title
Critical Anti-CRISPR Locus Repression by a Bi-functional Cas9 Inhibitor

Journal
Cell Host & Microbe, 28(1)

ISSN
1931-3128

Authors
Osuna, Beatriz A
Karambelkar, Shweta
Mahendra, Caroline
et al.

Publication Date
2020-07-01

DOI
10.1016/j.chom.2020.04.002

Peer reviewed

HHS Public Access

Author manuscript

Cell Host Microbe. Author manuscript; available in PMC 2021 July 08.

Published in final edited form as:

Cell Host Microbe. 2020 July 08; 28(1): 23–30.e5. doi:10.1016/j.chom.2020.04.002.

Critical anti-CRISPR locus repression by a bi-functional Cas9 inhibitor

Beatriz A. Osuna[1], **Shweta Karambelkar**[1], **Caroline Mahendra**[1], **Anne Sarbach**[2], **Matthew C. Johnson**[1], **Samuel Kilcher**[2,*], **Joseph Bondy-Denomy**[1,3,4,5,*]

[1]Department of Microbiology and Immunology, University of California, San Francisco, San Francisco, CA 94158, USA [2]Institute of Food, Nutrition, and Health, ETH Zurich, Zurich CH 8092, Switzerland [3]Quantitative Biosciences Institute, University of California, San Francisco, San Francisco, CA 94158, USA [4]Innovative Genomics Institute, Berkeley, CA, USA [5]Lead Contact

SUMMARY

Bacteriophages must rapidly deploy anti-CRISPR proteins (Acrs) to inactivate the RNA-guided nucleases that enforce CRISPR-Cas adaptive immunity in their bacterial hosts. *Listeria monocytogenes* temperate phages encode up to three anti-Cas9 proteins, with *acrIIA1* always present. AcrIIA1 inhibits Cas9 with its C-terminal domain; however, the function of its highly conserved N-terminal domain (NTD) is unknown. Here, we report that the AcrIIA1^{NTD} is a critical transcriptional repressor of the anti-CRISPR promoter. The strong anti-CRISPR promoter generates a rapid burst of transcription during phage infection and the subsequent negative feedback from AcrIIA1^{NTD} is required for optimal phage replication, even in the absence of CRISPR-Cas immunity. In the presence of CRISPR-Cas immunity, the AcrIIA1 two-domain fusion acts as a "Cas9 sensor," tuning *acr* expression according to Cas9 levels. Finally, we identify AcrIIA1^{NTD} homologues in other *Firmicutes*, and demonstrate that they have been co-opted by hosts as "anti-anti-CRISPRs," repressing phage anti-CRISPR deployment.

eTOC

Bacterial viruses (phages) infecting *Listeria* encode a suite of "anti-CRISPR" (Acr) proteins that inhibit Cas9 immunity. Osuna et al. show that AcrIIA1 is both an autorepressor, silencing the strong *acr* promoter is key for phage fitness, *and* binds to Cas9, allowing phages to tune Acr expression to match Cas9 levels.

[*]**Contact Information:** Correspondence: Samuel Kilcher (samuel.kilcher@hest.ethz.ch) and Joseph Bondy-Denomy (joseph.bondy-denomy@ucsf.edu).

AUTHOR CONTRIBUTIONS

B.A.O., S.Ki., and J.B.-D. conceived and designed the study. B.A.O., S.Ka., C.M., A.S., S.Ki., M.J., and J.B.-D. performed experiments. S.Ki., and J.B.-D. supervised experiments. All authors evaluated results. B.A.O. and J.B.-D. wrote the manuscript with input from all authors.

DECLARATION OF INTERESTS

J.B.-D. is a scientific advisory board member of SNIPR Biome and Excision Biotherapeutics and a scientific advisory board member and co-founder of Acrigen Biosciences, and is an inventor on patents relating to anti-CRISPR proteins.

Graphical Abstract

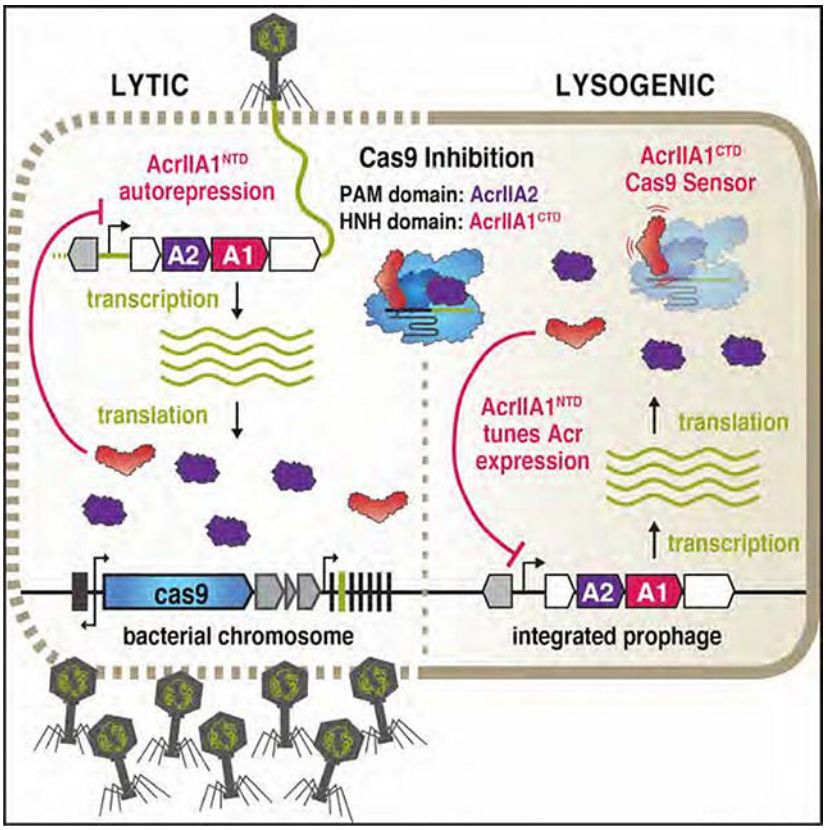

INTRODUCTION

The constant battle for survival between bacterial predators (phages) and their hosts has led to the evolution of numerous defensive and offensive strategies in both phages and bacteria (Stern and Sorek, 2011). Bacteria employ various mechanisms to combat phages, including CRISPR-Cas adaptive immune systems that keep a record of past viral infections in a CRISPR array with phage DNA fragments (spacers) stored between repetitive DNA sequences (Mojica et al., 2005). These spacers are transcribed into CRISPR RNAs (crRNAs), which bind CRISPR-associated (Cas) proteins to guide the sequence-specific detection and nucleolytic destruction of infecting phage genomes (Brouns et al., 2008; Garneau et al., 2010).

To evade this bacterial immunity, phages have evolved many tactics, including anti-CRISPR (Acr) proteins (Borges et al., 2017). Anti-CRISPRs are highly diverse and share no protein characteristics in common; they contain distinct amino acid sequences structures (Hwang and Maxwell, 2019; Trasanidou et al., 2019). However, the anti-CRISPR genomic locus displays some recurring features, containing up to three small anti-CRISPR genes and a signature anti-CRISPR-associated (*aca*) gene within a single operon (Borges et al., 2017). *aca* genes are almost invariably present in anti-CRISPR loci and they encode repressor

proteins that contain a characteristic helix-turn-helix (HTH) DNA-binding motif (Birkholz et al., 2019; Stanley et al., 2019).

Listeria monocytogenes prophages contain a unique anti-CRISPR locus without an obvious standalone *aca* gene. These phages do, however, encode *acrIIA1*, a signature anti-CRISPR gene, which contains an HTH motif in its N-terminal domain (NTD) (Rauch et al., 2017). The AcrIIA1 HTH motif is highly conserved across orthologues, yet it is completely dispensable for anti-CRISPR activity, which resides in the C-terminal domain (CTD) (companion manuscript; Osuna et al., 2020a). Thus, the role and function of the AcrIIA1^{NTD} remains unknown. Here, we show that AcrIIA1 is a bi-functional anti-CRISPR protein that performs a crucial regulatory role as an autorepressor of *acr* locus transcription that is required for optimal phage fitness. AcrIIA1^{NTD} orthologues in phages and plasmids across the *Firmicutes* phylum also display autorepressor activity. We also show that the bacterial host can exploit the highly conserved anti-CRISPR locus repression mechanism, using the AcrIIA1^{NTD} as an "anti-anti-CRISPR" to block phage anti-CRISPR expression during phage infection and lysogeny.

RESULTS

AcrIIA1^{NTD} promotes general lytic growth and prophage induction

While interrogating anti-CRISPR phages in *Listeria*, we observed that two phage mutants displayed a lytic replication defect when their anti-CRISPR locus was deleted (ΦJ0161aΔ*acrIIA1–2* and ΦA006Δ*acr*), even in a host lacking Cas9 (Figure 1A and 1B). The only gene that was removed from both phages was *acrIIA1*, suggesting that aside from acting as an anti-CRISPR, AcrIIA1 is also generally required for optimal phage replication. AcrIIA1 is a two-domain protein with a CTD that inhibits Cas9 (companion manuscript; Osuna et al., 2020a) and an NTD of uncharacterized function that contains a helix-turn-helix (HTH) motif similar to known transcriptional repressors (Ka et al., 2018). We hypothesized that the putative transcriptional repressor activity of AcrIIA1^{NTD} is necessary for phage replication, even in the absence of CRISPR-Cas immunity. Indeed, complementation with *acrIIA1^{NTD} in trans* rescued the lytic growth defects of both phages containing anti-CRISPR locus deletions (Figure 1A and 1B). Rare spontaneous mutants (~10^{-5} frequency) of the ΦJ0161aΔ*acrIIA1–2* phage that grew in the absence of *acrIIA1^{NTD}* complementation were isolated, revealing that mutations in the −35 and −10 promoter elements suppressed the growth defect, as did a large deletion of the region, consistent with a vital *cis*-acting role for AcrIIA1 (Figure 1C).

A panel of ΦA006-derived phages engineered to study anti-CRISPR deployment during phage infection (see companion manuscript; Osuna et al., 2020a) was next examined in a host lacking Cas9. The lytic growth defect was again apparent in each phage that lacked AcrIIA1 or AcrIIA1^{NTD} and providing *acrIIA1^{NTD} in trans* or *in cis* (i.e. encoded in the phage *acr* locus) ameliorated this growth deficiency (Figure 1B and S1A). The phage engineered to express *acrIIA1^{CTD}* alone (ΦA006-IIA1^{CTD}), which is naturally always fused to *acrIIA1^{NTD}*, displayed the strongest lytic defect amongst the ΦA006 phages and generated minuscule plaques (see spot titration, Figure 1B). The plaque size and phage titer deficiencies of ΦA006-IIA1^{CTD} were fully restored with *acrIIA1^{NTD}* supplemented *in trans*

and most notably, when *acrIIA1*^{NTD} was added to the phage genome as a separate gene (ΦA006-IIA1$^{NTD+CTD}$, Figure 1B). Together, these data suggest that the HTH-containing AcrIIA1^{NTD} enacts an activity that is a key determinant of phage fitness, irrespective of CRISPR-Cas immunity.

To test whether AcrIIA1^{NTD} is also important during lysogeny, prophages were induced with mitomycin C treatment and the resulting phage titer was assessed. The ΦJ0161aΔ*acrIIA1–2* prophage displayed a strong induction deficiency, yielding 25-fold less phage, compared to the WT prophage or the *acrIIA1*-complemented mutant (Figure 1D). Attempts to efficiently induce ΦA006 prophages were unsuccessful, as previously observed (Loessner, 1991; Loessner et al., 1991). Therefore, AcrIIA1 is a bi-functional protein that not only acts as an anti-CRISPR, but also plays a critical role in the phage life cycle, promoting optimal lytic replication and lysogenic induction irrespective of CRISPR-Cas9.

AcrIIA1^{NTD} is a repressor of the *anti-CRISPR* promoter and a Cas9 "sensor"

The AcrIIA1^{NTD} domain bears close structural similarity to the phage 434 cI protein (Ka et al., 2018), an autorepressor that binds specific operator sequences in its own promoter (Johnson et al., 1981). Analysis of the anti-CRISPR promoters in ΦA006, ΦJ0161, and ΦA118 revealed a conserved palindromic operator sequence (Figures 2A and S2A), suggesting transcriptional control by a conserved regulator such as AcrIIA1. An RFP transcriptional reporter assay showed that full-length AcrIIA1 and AcrIIA1^{NTD}, but not AcrIIA1^{CTD}, repress the ΦA006 anti-CRISPR promoter (Figure 2B, left panel). *In vitro* MST binding assays also confirmed that AcrIIA1 (K_D = 26 ± 10 nM) or AcrIIA1^{NTD} (K_D = 28 ± 3 nM), but not the AcrIIA1^{CTD}, bind the anti-CRISPR promoter with high affinity (Figures 2C and S2B). Moreover, mutagenesis of the terminal nucleotides of the palindromic operator sequence prevented AcrIIA1-mediated repression of the ΦA006 anti-CRISPR promoter (Figure 2B, right panel) and abolished promoter binding *in vitro* (Figure 2C). Alanine scanning mutagenesis of conserved residues predicted to be important for DNA binding and dimerization (Ka et al., 2018) identified AcrIIA1^{NTD} residues L10, T16, and R48 as critical for transcriptional repression, whereas AcrIIA1^{CTD} mutations had little effect (Figure 2D). These data show that AcrIIA1^{NTD} represses anti-CRISPR transcription by binding a highly conserved operator, and together with the suppressors isolated above, we conclude that this repression is important due to the need to silence a strong promoter (see Discussion).

We next hypothesized that the ability of AcrIIA1 to repress transcription with one domain and inactivate Cas9 with another would enable the tuning of *acr* transcripts to match the levels of Cas9 in the native host, *L. monocytogenes*. A reporter lysogen was engineered by inserting a *nanoluciferase* (*nluc*) gene in the *acr* locus. Low *acr* expression was seen in the absence of Cas9, or during low levels of Cas9 expression, however *acr* reporter levels increased by ~5-fold when Cas9 was overexpressed (Figure 2E, left). *acr* induction was not seen in the absence of AcrIIA1^{CTD} (Figure 2E, right), the Cas9 binding-domain, supporting a model where Cas9 "sensing" de-represses the *acr* promoter. After confirming de-repression through an increase in Cas9 levels, we sought to confirm that AcrIIA1^{NTD} is also capable of further repressing lysogenic anti-CRISPR expression. We therefore expressed the

AcrIIA1^{NTD} repressor *in trans* and assessed anti-CRISPR function. The Cas9 degradation normally induced by prophage-expressed AcrIIA1 activity (companion manuscript; Osuna et al., 2020a) was successfully prevented by AcrIIA1^{NTD} (Figure 2F). These data collectively demonstrate that AcrIIA1 autoregulates *acr* transcript levels in *L. monocytogenes* and can increase *acr* expression in response to increased Cas9 expression.

Transcriptional autoregulation is a general feature of the AcrIIA1 superfamily

Recent studies have reported transcriptional autoregulation of anti-CRISPR loci by HTH-proteins in mobile genetic elements of Gram-negative *Proteobacteria* (Birkholz et al., 2019; Stanley et al., 2019). To determine whether anti-CRISPR locus regulation is similarly pervasive amongst mobile genetic elements in the Gram-positive *Firmicutes* phylum, we assessed AcrIIA1 homologs for transcriptional repression of their predicted cognate promoters and our model ΦA006 phage promoter. Homologs sharing 21% (i.e. Lmo *orfD*) to 72% amino acid sequence identity with AcrIIA1^{NTD} were selected from mobile elements in *Listeria, Enterococcus, Leuconostoc,* and *Lactobacillus* (Figure 3A and S3A). All AcrIIA1 homologs repressed transcription of their cognate promoters by 42–99%, except AcrIIA1 from *Lactobacillus parabuchneri,* where promoter expression was undetectable (Figures 3A and S3B). Strong repression of the model ΦA006 promoter was only enacted by *Listeria* orthologues possessing ≥68% protein sequence identity (Figure 3A). Likewise, AcrIIA1$_{ΦA006}$ only repressed the promoters associated with orthologues that repressed the ΦA006 promoter (Figure 3B). Interestingly, an AcrIIA1^{NTD} palindromic binding site resides in the protein-coding sequence of the AcrIIA1$_{LMO10}$ homolog, which displayed no anti-CRISPR activity despite possessing 85% AcrIIA1^{CTD} sequence identity (Figures 3C and S3A). When this AcrIIA1^{NTD} binding site was disrupted with silent mutations, AcrIIA1$_{LMO10}$ anti-CRISPR function manifested (Figure 3C), confirming that intragenic anti-CRISPR repression can also occur. Altogether, these findings demonstrate that the anti-CRISPR promoter-AcrIIA1^{NTD} repressor relationship is highly conserved and likely performs a vital repressive function in these diverse mobile genetic elements.

Host-encoded AcrIIA1^{NTD} blocks phage anti-CRISPR deployment

AcrIIA1^{NTD} orthologues are encoded by many *Firmicutes* including *Enterococcus, Bacillus, Clostridium, and Streptococcus* (Rauch et al., 2017). In most cases, AcrIIA1^{NTD} is fused to distinct AcrIIA1^{CTDs} in mobile genetic elements, which are likely anti-CRISPRs that inhibit CRISPR-Cas systems in their respective hosts. Interestingly, there are instances where core bacterial genomes encode AcrIIA1^{NTD} orthologues that are short ~70–80 amino acid proteins possessing only the HTH domain. One example is in *Lactobacillus delbrueckii*, where strains contain an AcrIIA1^{NTD} homolog (35% identical, 62% similar to AcrIIA1$_{ΦA006}$) with key residues conserved (e.g. L10 and T16). Given that AcrIIA1^{NTD} represses anti-CRISPR transcription, we wondered whether bacteria could co-opt this regulator and exploit its activity *in trans*, preventing a phage from deploying its anti-CRISPR arsenal. Remarkably, we observed that the *L. delbrueckii* AcrIIA1^{NTD} homolog is always a genomic neighbor of either the Type I-E, I-C, or II-A CRISPR-Cas systems in this species (Figure 4A), and these CRISPR-associated AcrIIA1^{NTD} proteins are highly conserved (>95% sequence identity). This association is supportive of an “anti-anti-CRISPR” role that aids CRISPR-Cas function by repressing the deployment of phage inhibitors against each

system. Although there are no specific anti-CRISPR proteins identified in *Lactobacillus* phages and prophages that express anti-CRISPRs, we reasoned that phages with their own *acrIIA1* homolog might have *acr* loci that would be vulnerable to repression by the host protein. Fluorescent reporters were built, driven by seven different *Lactobacillus* phage or prophage promoters that possess an *acrIIA1* homolog in their downstream operon (Figure S3C). This enabled the identification of one promoter, from phage Lrm1, that was robustly repressed by *L. delbrueckii* host AcrIIA1^{NTD}. This confirms that a *bona fide acr* locus in a *Lactobacillus* phage can be repressed by a host version of a hijacked *acr* repressor (Figure 4B).

To interrogate the anti-anti-CRISPR prediction in a native phage assay, we expressed AcrIIA1^{NTD} from a plasmid (Figure 4B and S4B) or from an integrated single-copy *acrIIA1*^{NTD} driven by its cognate phage promoter (Figure S4B) in *L. monocytogenes*. A panel of distinct anti-CRISPR-encoding phages became vulnerable to Cas9 targeting when AcrIIA1^{NTD} was expressed by the host (Figures 4C and S4B), whereas expression of full-length AcrIIA1, AcrIIA1^{CTD}, or AcrIIA4 had the expected anti-CRISPR phenotype (Figures 4C and S4A). Each of these phages possesses complete or partial spacer matches to the *Lmo*10403s CRISPR array. In contrast, replication of the non-targeted phages, ΦJ0161a (Figure 4C) and ΦP35 (Figure S4B), was unperturbed. Additionally, the *acr::nluc* reporter phage was used in a similar experiment, confirming that *acr* expression rapidly occurs during infection and can be silenced by expression of AcrIIA1 or AcrIIA1^{NTD} (Figure 4D), while a model late promoter (*ply::nluc*) was not silenced (Figure 4E). These data demonstrate that hosts can use the anti-CRISPR repressor to block anti-CRISPR synthesis, rendering a phage unable to express its Acr proteins.

DISCUSSION

The *Listeria* phage anti-CRISPR AcrIIA1 was first described as a Cas9 inhibitor, and here we demonstrate that it is also a transcriptional autorepressor of the *acr* locus required for optimal lytic growth and prophage induction. Notably, this bi-functional regulatory anti-CRISPR has the ability to tune *acr* transcription in accordance with Cas9 levels.

Transcriptional autorepression is seemingly the predominant regulatory mechanism in bacteria and phages, as 40% of transcription factors in *E. coli* exert autogenous negative control (Thieffry et al., 1998). Due to their short response times, negative autoregulatory circuits are thought to be particularly advantageous in dynamic environments where rapid responses improve fitness. A strong promoter initially produces a rapid rise in transcript levels and after some time, repressor concentration reaches a threshold, shutting off its promoter to maintain steady-state protein levels (Madar et al., 2011; Rosenfeld et al., 2002). During infection, phages must rapidly produce anti-CRISPR proteins to neutralize the preexisting CRISPR-Cas complexes in their bacterial host. Consistent with the rapid response times exhibited by negatively autoregulated promoters, we observed a burst of anti-CRISPR locus expression within ten minutes post infection using a reporter phage (Figures 4C and S4C). During lysogeny, autorepression by AcrIIA1 presumably tempers anti-CRISPR locus expression, generating steady-state anti-CRISPR levels to maintain Cas9 inactivation.

Negative autoregulation maintains precise levels of the proteins encoded by the operon to prevent toxic effects caused by their overexpression (Thieffry et al., 1998), as classically observed with the λ phage genes cII and N (Shimatake and Rosenberg, 1981). In this study, the engineered ΦA006-IIA1^{CTD} phage, which only contains the AcrIIA1^{CTD} and lacks the AcrIIA1^{NTD} autorepressor, displayed a pronounced lytic growth defect, even stronger than the defect of the ΦA006$^{\Delta acr}$ phage that completely lacks anti-CRISPRs (Figure 1B). This suggests that the AcrIIA1^{NTD} autoregulatory domain is fused to AcrIIA1^{CTD} in nature to limit the expression of an anti-CRISPR domain that can be toxic to the phage. Phages expressing only AcrIIA4 or AcrIIA12 were only mildly affected by the absence of AcrIIA1^{NTD} (Figure 1B). However, other *Listeria* phage anti-CRISPRs (such as AcrIIA3) have been shown to exert toxic effects (Rauch et al., 2017), underscoring the need for an autoregulatory mechanism that tempers anti-CRISPR levels. The ΦJ0161a phage displays a remarkably strong growth defect when AcrIIA1 is absent (ΦJ0161aΔ*acrIIA1–2*, Figure 1A), which is suppressed by promoter mutations or deletion of *orfA* (Figure 1C), suggesting that misregulation of a gene within the *acr* locus may be deleterious. Constitutively strong promoter activity may also have other deleterious effects. A recent study demonstrated that neighboring phage genes can be temporally misregulated in the absence of an anti-CRISPR locus autorepressor, Aca1 (Stanley et al., 2019).

Beyond *cis* regulatory auto-repression, prophages may also use AcrIIA1^{NTD} to combat phage superinfection, benefitting both the prophage and host cell. The phage lambda cI protein, for example, represses prophage lytic genes and prevents superinfection by related phages during lysogeny (Johnson et al., 1981). Similarly, a lysogen could use AcrIIA1^{NTD} to bolster the activity of a second CRISPR-Cas system in its host (such as the Type I-B system that is common in *Listeria*) by preventing incoming phages from expressing their Type I-B anti-CRISPRs. Host expressed AcrIIA1^{NTD} does manifest as an anti-anti-CRISPR, blocking anti-CRISPR expression from infecting or integrated phages (Figures 4B and S4B). We also demonstrate that AcrIIA1^{NTD} orthologues that reside in non-mobile regions of bacterial genomes can perform as a *bona fide* anti-CRISPR repressor. Thus, the importance of the conserved anti-CRISPR locus repression mechanism may represent a weakness in the phage, which can be exploited by the host through the co-opting of this anti-CRISPR regulator.

STAR METHODS

RESOURCE AVAILABILITY

Lead Contact—Please direct any requests for further information or reagents to the lead contact, Joseph Bondy-Denomy (joseph.bondy-denomy@ucsf.edu).

Materials Availability—*Listeria* strains, plasmids, and phages constructed and used in this study are disclosed in Table S2 (Excel spreadsheet).

EXPERIMENTAL MODEL AND SUBJECT DETAILS

Microbe Strains—*Listeria monocytogenes* strains (10403s) were cultured in brain-heart infusion (BHI) medium at 30°C. To ensure plasmid maintenance in *Listeria* strains, BHI was supplemented with tetracycline (2 μg/mL) for pPL2oexL integrated constructs or

erythromycin (7.5 μg/mL) for pLEB579-derived constructs. *Escherichia coli* (DH5α, XL1Blue, NEB 10-beta, or NEB Turbo for plasmid maintenance and SM10 for conjugation into *Listeria*) and *Pseudomonas aeruginosa* (PAO1) were cultured in LB medium at 37°C. To maintain plasmids, LB was supplemented with chloramphenicol (25 μg/mL) for pPL2oexL in *E. coli*, erythromycin (250 μg/mL) for pLEB579 in *E. coli,* gentamicin (30 μg/mL) for pHERD30T in *E. coli* and *P. aeruginosa*, or carbenicillin (250 μg/mL for *P. aeruginosa,* 100 μg/mL for *E. coli*) for pMMB67HE. For maintaining pHERD30T and pMMB67HE in the same *P. aeruginosa* strain, media was supplemented with 30 μg/mL gentamicin and 100 μg/mL carbenicillin. The *Listeria* strains, plasmids, and phages constructed and used in this study are listed in Table S2.

Phages—*Listeria* phages A006, A118, A502, A620, J0161a, P35, and their derivatives were all propagated at 30°C on *acrIIA1*^{NTD}-expressing *L. monocytogenes* 10403sϕcure (*Δcas9*, Δ*tRNAArg::pPL2oexL-acrIIA1*^{NTD}) to allow optimal lytic growth of phages lacking their own *acrIIA1*^{NTD}. The *Pseudomonas* DMS3m-like phage (JBD30) was propagated on PAO1 at 37°C. All phages were stored in SM buffer (100 mM NaCl, 8 mM $MgSO_4$•$7H_2O$, 50 mM Tris-HCl pH 7.5, 0.01% (w/v) gelatin), supplemented with 10 mM $CaCl_2$ for *Listeria* phages, at 4°C.

METHOD DETAILS

***Listeria* and *Pseudomonas* strain construction—**DNA fragments were PCR-amplified from genomic, plasmid, or synthesized DNA and cloned by Gibson Assembly into *Listeria* plasmids: episomal pLEB579 (Beasley et al., 2004) or the pPL2oexL single-copy integrating plasmid derived from pPL2 (Lauer et al., 2002) or *P. aeruginosa* plasmids: pMMB67HE or pHERD30T. To generate all *Listeria monocytogenes* strains, pPL2oexL plasmids were conjugated (Lauer et al., 2002; Simon et al., 1983) and pLEB579 plasmids were electroporated (Hupfeld et al., 2018; Park and Stewart, 1990) into *Lmo*10403s. For all *Pseudomonas* strains, plasmids were electroporated into PAO1 (Choi et al., 2006).

Isogenic ϕA006 anti-CRISPR phage engineering—Isogenic ϕA006 phages encoding distinct anti-CRISPRs from the native anti-CRISPR locus were engineered by *in vitro*-assemby of synthetic bacteriophage DNA as subsequent genome activation in *L. monocytogenes* L-form cells (EGDe strain variant Rev2) as previously described (Kilcher et al., 2018). Denoted *acr* genes (*) contain the strong ribosomal binding site (RBS) naturally associated with the first gene in the natural ϕA006 anti-CRISPR locus (*orfA*) whereas unmarked genes contain their native RBS. Note: the *acrIIA1* RBS is weaker than the *orfA* RBS. The reporter phage ϕA006_acr::*nluc* was constructed by inserting a codon-optimized [optimized for *L. monocytogenes* using JCat (Grote et al., 2005)] nanoluciferase (*nluc*) gene sequence upstream of *acrIIA1* using the endogenous *acrIIA1* RBS (gene synthesis: ThermoFisher). DNA sequence of codon-optimized nanoluciferase (5'–3'):

ATGGTTTTCACTTTAGAAGATTTCGTTGGTGATTGGCGTCAAACTGCTGGTTACAA
CTTAGATCAAGTTTTAGAACAAGGTGGTGTTTCTTCTTTATTCCAAAACTTAGGTG
TTTCTGTTACTCCAATCCAACGTATCGTTTTATCTGGTGAAAACGGTTTAAAAATC
GATATCCATGTTATCATCCCATACGAAGGTTTATCTGGTGATCAAATGGGTCAAATC

GAAAAAATCTTCAAAGTTGTTTACCCAGTTGATGATCATCATTTCAAAGTTATCTT
ACATTACGGTACTTTAGTTATCGATGGTGTTACTCCAAACATGATCGATTACTTCGG
TCGTCCATACGAAGGTATCGCTGTTTTCGATGGTAAAAAAATCACTGTTACTGGTA
CTTTATGGAACGGTAACAAAATCATCGATGAACGTTTAATCAACCCAGATGGTTCT
TTATTATTCCGTGTTACTATCAACGGTGTTACTGGTTGGCGTTTATGTGAACGTATC
TTAGCTTAA

***Listeria* phage titering—**A mixture of 150 μl stationary *Listeria* culture and 3 mL molten LC top agar (10 g/L tryptone, 5 g/L yeast extract, 10 g/L glucose, 7.5 g/L NaCl, 10 mM $CaCl_2$, 10 mM $MgSO_4$, 0.5% agar) was poured onto a BHI plate (1.5% agar) to generate a bacterial lawn, 3 μL of phage ten-fold serial dilutions were spotted on top, and after 24 hr incubation at 30°C, plate images were collected using the Gel Doc EZ Documentation system (BioRad) and Image Lab (BioRad) software.

Quantification of phage plaque forming units—*Listeria* phage infections were conducted using the soft agar overlay method: 10 μL phage dilution was mixed with 150 μL stationary *Listeria* culture in 3 mL molten LC top agar supplemented with 300 μg/mL Tetrazolium Violet (TCI Chemicals) to generate contrast for plaque visualization (Hurst et al., 1994) and poured onto a BHI-agar plate. After 24 hr incubation at 30°C, phage plaque-forming units (PFU) were quantified.

Isolation of J0161Δacr suppressor phages—A high titer lysate of the J0161Δ*acrIIA1–2* was plated on Δ*cas9* strains that do not express *acrIIA1*. This caused a reduction in apparent titer by ~5 orders of magnitude but low frequency plaques were picked and propagated through three rounds of plaque purification. After plaque purification, the *acr* locus was PCR amplified from phage DNA and amplicons were Sanger sequenced to identify mutations.

Construction of *Listeria* lysogens—Lysogens were isolated from plaques that emerged after titering phages (ϕJ0161a, ϕA006, or their derivatives) on a lawn of *Lmo*10403sϕcure*Δcas9* or *Lmo*EGD-e (see "*Listeria* phage titering"). Lysogeny was confirmed by prophage induction with mitomycin C (0.5 μg/mL) treatment as previously described (Estela et al., 1992) and by PCR amplification and Sanger sequencing of the phage anti-CRISPR locus. All *Lmo*10403s strains containing prophages were lysogenized and verified prior to introducing additional constructs (integrated pPL2oexL or episomal pLEB579).

***Listeria* reporter phage assays—**To quantify *acr*-locus expression during lytic infection, over-night cultures of the indicated host cells were diluted to an OD_{600}=0.01 and infected with ϕA006 *acr::nluc* at an MOI=1. Time-course infection assays were performed at 30°C. At indicated time-points, 20 μL was removed from the infection, mixed with 20 μL Nano-GLO substrate, and bioluminescence quantified on a Glo-Max NAVIGATOR device (Promega, integration time = 5 s). Relative luminescence units (RLUs) were background corrected (luminescence of a phage-only control) and divided by values of a control infection with wild-type ϕA006. ϕA006 *acr::nluc* lysogens were produced as described in "construction of *Listeria* lysogens" and confirmed by PCR (Primer1:

TAATTTGCTTAACTGATACC; Primer2: TGACTACTACGTATATTCG), by measuring bioluminescence, and by assessing homo-immunity. To quantify *acr*-locus expression from ϕA006 *acr::nluc* lysogens, log-phase cultures were diluted to an OD_{600}=0.05 and bioluminescence quantified and divided by background values obtained from non-lysogenized parental strains.

Prophage induction efficiency quantification—Prophages were induced from *Lmo*10403s::ΦJ0161 lysogens expressing *cis-acrIIA1* from the prophage Acr locus or *trans-acrIIA1* from the bacterial host genome by treating with 0.5 μg/mL mitomycin C as previously described (Estela et al., 1992). After overnight incubation with continuous shaking at 30°C, cells were pelleted by centrifugation at 8000 g for 10 min and phage-containing supernatants were harvested. To quantify the amount of phage induced from each lysogen, phage-containing supernatants were used to infect *Lmo*10403sΦcure lacking *cas9* and expressing $AcrIIA1^{NTD}$ (*Δcas9;IIA1*^{NTD}, to bypass the lytic growth defect of ΦJ0161Δ*acrIIA1–2*) as described in "plaque forming unit (PFU) quantification of *Listeria* phages" and the resulting PFUs were quantified. Data are displayed as the mean PFU/mL after prophage induction of four biological replicates ± SD (error bars).

***acr* promoter transcriptional repression—**To generate *acr* promoter transcriptional reporters, the nucleotide sequences (~100–350 base pairs) upstream of putative *acr* loci encoding *acrIIA1* homologs were synthesized (Twist Bioscience) and cloned upstream of an mRFP gene into the pHERD30T vector. Promoter sequences are listed in Table S1. Transcriptional reporters were electroporated into *P. aeruginosa* PAO1 strains containing pMMB67HE-AcrIIA1-variants. Saturated overnight cultures of *Pseudomonas* were diluted 1:10 in LB supplemented with 30 μg/mL gentamicin, 100 μg/mL carbenicillin, and 1 mM IPTG to induce AcrIIA1 expression in a 96-well special optics microplate (Corning). *C*ells were incubated at 37°C with continuous double-orbital rotation for 24 hr in the Synergy H1 Hybrid Multi-Mode Reader (BioTeK) and measurements of OD_{600} and RFP (excitation 555 nm, emission 610 nm) relative fluorescence units (RFU) recorded every 5 min with the Gen5 (BioTek) software. Background fluorescence of growth media was subtracted and the resulting RFU values were normalized to OD_{600} ($\frac{RFU - background}{OD_{600}}$). Data are displayed as the mean normalized fluorescence of three biological replicates ± SD. Data are shown as the mean percentage RFP repression (RFU values at 960 min for AcrIIA1 mutants and 1170 min for homologs, normalized to OD_{600}) in the presence of AcrIIA1 relative to controls lacking AcrIIA1 of at least three biological replicates ± SD (error bars).

Acr protein expression and purification—N-terminally 6xHis-tagged Acr proteins were expressed from the pET28 vector. Recombinant protein expression was induced with 0.25 mM isopropyl β-D-1-thiogalactopyranoside (IPTG) at 18 °C overnight. Cells were harvested by centrifugation and lysed by sonication in buffer A (50 mM Tris-HCl pH 7.5, 500 mM NaCl, 0.5 mM DTT, 20 mM imidazole, 5% glycerol) supplemented with 1 mM PMSF and 0.25 mg/mL lysozyme (Sigma). Cell debris was removed by centrifugation at 20000 g for 40 min at 4 °C and the lysate incubated with Ni-NTA Agarose Beads (Qiagen). After washing, bound proteins were eluted with Buffer A containing 300 mM imidazole and

dialyzed overnight into storage buffer (20 mM HEPES-NaOH pH 7.4, 150mM KCl, 10% glycerol, 2mM DTT).

***in vitro* AcrIIA1–anti-CRISPR promoter binding—**The affinities of AcrIIA1 and individual domains for DNA were measured in triplicate using microscale thermophoresis (MST) on the Monolith NT.115 instrument (NanoTemper Technologies GmbH, Munich, Germany). Single-stranded complementary oligonucleotides were annealed to generate 40 bp *acr* promoter fragments harboring WT or mutated palindrome. The DNA substrate at 0.15 nM to 5 μM concentrations was incubated with 12.5 nM RED-tris-NTA-labeled AcrIIA1/ domains at room temperature for 10 min in 1x buffer (50 mM Tris-HCl pH 7.4, 150 mM NaCl, 10 mM MgCl2, 0.05 % Tween-20). Samples were loaded into Monolith NT.115 Capillaries and measurements were performed at 25 °C using 40% LED power and medium microscale thermophoresis power. Data analyses were carried out using NanoTemper analysis software. DNA substrate sequences used are as follows:

5’-AACTATTGAC**TACTACG**TATATT**CGTAGTA**TAATGTGAAT-3’ (Wild-type)

5’-AACTATTGAC**A**ACTACGTATATT**CGTAGTT**TAATGTGAAT-3’ (Terminal Mutations)

5’-AACTATTGAC**A**AC**A**AC**C**TATATT**G**GT**T**GT**T**TAATGTGAAT-3’ (Six Mutations)

***Listeria* protein samples for immunoblotting—**Saturated overnight cultures of *Lmo*10403s strains overexpressing FLAG-tagged Cas9 (*Δcas9,* Δ*tRNAArg::pPL2oexL-LmoCas9–6xHis-FLAG*) were diluted 1:10 in BHI with appropriate antibiotic selection (see “microbes”), grown to log phase (OD_{600} 0.2–0.6), 1.6 OD_{600} units of cells were harvested by centrifugation at 8000 g for 5 min at 4°C. Cells were lysed with lysozyme treatment: cell pellets were resuspended in 200 μL of TE buffer supplemented with 2.5 mg/mL lysozyme and 1x cOmplete mini EDTA-free protease inhibitor cocktail (Roche), samples were incubated at 37°C for 30 min, quenched with one-third volume of 4X Laemmli Sample Buffer (Bio-Rad), and boiled for 5 min at 95°C.

Immunoblotting—Protein samples were separated by SDS-PAGE using 4–20% Mini-PROTEAN TGX gels (BioRad) and transferred in 1X Tris/Glycine Buffer onto 0.22 micron PVDF membrane (Bio-Rad). Blots were probed with the following antibodies diluted 1:5000 in 1X TBS-T containing 5% nonfat dry milk: rabbit anti-FLAG (Sigma-Aldrich Cat# F7425, RRID:AB_439687), mouse anti-FLAG (Sigma-Aldrich Cat# F1804, RRID:AB_262044), HRP-conjugated goat anti-Rabbit IgG (Bio-Rad Cat# 170–6515, RRID:AB_11125142), and HRP-conjugated goat anti-mouse IgG (Santa Cruz Biotechnology Cat# sc-2005, RRID:AB_631736). Blots were developed using Clarity ECL Western Blotting Substrate (Bio-Rad) and chemiluminescence was detected on an Azure c600 Imager (Azure Biosystems).

QUANTIFICATION AND STATISTICAL ANALYSIS

All numerical data, with the exception of the microscale thermophoresis (MST) data, were analyzed and plotted using GraphPad Prism 6.0 software. The MST data were analyzed

using the NanoTemper analysis software (NanoTemper Technologies GmbH) and plotted using GraphPad Prism 6.0 software. Statistical parameters are reported in the Figure Legends.

Data and Code Availability—The AcrIIA1 homolog protein accession numbers and associated promoter sequences are disclosed in Table S1.

Supplementary Material

Refer to Web version on PubMed Central for supplementary material.

ACKNOWLEDGEMENTS

We would like to thank Daniel A. Portnoy (UC Berkeley) for providing the pLMB3C-pRhamnose plasmid, and Jonathan Asfaha (David Morgan Lab, UCSF) and Ujjwal Rathore (Alex Marson Lab, UCSF) for experimental advice and reagents. The J.B.-D lab was supported by the UCSF Program for Breakthrough Biomedical Research funded in part by the Sandler Foundation, the Searle Fellowship, the Vallee Foundation, the Innovative Genomics Institute, an NIH Director's Early Independence Award DP5-OD021344, and NIH R01GM127489. The S.Ki. lab was supported by an Ambizione Fellowship (Swiss National Science Foundation, PZ00P3_174108).

REFERENCES

Beasley SS, Takala TM, Reunanen J, Apajalahti J, and Saris PEJ (2004). Characterization and Electrotransformation of Lactobacillus Crispatus Isolated from Chicken Crop and Intestine. Poult. Sci. 83, 45–48. [PubMed: 14761083]

Birkholz N, Fagerlund RD, Smith LM, Jackson SA, and Fineran PC (2019). The autoregulator Aca2 mediates anti-CRISPR repression. Nucleic Acids Res. 47, 9658–9665. [PubMed: 31428783]

Borges AL, Davidson AR, and Bondy-Denomy J (2017). The Discovery, Mechanisms, and Evolutionary Impact of Anti-CRISPRs. Annu. Rev. Virol. 4, null.

Brouns SJJ, Jore MM, Lundgren M, Westra ER, Slijkhuis RJH, Snijders APL, Dickman MJ, Makarova KS, Koonin EV, and van der Oost J (2008). Small CRISPR RNAs Guide Antiviral Defense in Prokaryotes. Science 321, 960–964. [PubMed: 18703739]

Choi K-H, Kumar A, and Schweizer HP (2006). A 10-min method for preparation of highly electrocompetent Pseudomonas aeruginosa cells: Application for DNA fragment transfer between chromosomes and plasmid transformation. J. Microbiol. Methods 64, 391–397. [PubMed: 15987659]

Estela LA, Sofos JN, and Flores BB (1992). Bacteriophage Typing of Listeria monocytogenes Cultures Isolated From Seafoods. J. Food Prot. 55, 13–17. [PubMed: 31071804]

Garneau JE, Dupuis M-È, Villion M, Romero DA, Barrangou R, Boyaval P, Fremaux C, Horvath P, Magadán AH, and Moineau S (2010). The CRISPR/Cas bacterial immune system cleaves bacteriophage and plasmid DNA. Nature 468, 67–71. [PubMed: 21048762]

Grote A, Hiller K, Scheer M, Münch R, Nörtemann B, Hempel DC, and Jahn D (2005). JCat: a novel tool to adapt codon usage of a target gene to its potential expression host. Nucleic Acids Res. 33, W526–W531. [PubMed: 15980527]

Hupfeld M, Trasanidou D, Ramazzini L, Klumpp J, Loessner MJ, and Kilcher S (2018). A functional type II-A CRISPR–Cas system from Listeria enables efficient genome editing of large non-integrating bacteriophage. Nucleic Acids Res. 46, 6920–6933. [PubMed: 30053228]

Hurst CJ, Blannon JC, Hardaway RL, and Jackson WC (1994). Differential Effect of Tetrazolium Dyes upon Bacteriophage Plaque Assay Titers. Appl Env. Microbiol 60, 3462–3465. [PubMed: 16349397]

Hwang S, and Maxwell KL (2019). Meet the Anti-CRISPRs: Widespread Protein Inhibitors of CRISPR-Cas Systems. CRISPR J. 2, 23–30. [PubMed: 31021234]

Johnson AD, Poteete AR, Lauer G, Sauer RT, Ackers GK, and Ptashne M (1981). λ Repressor and cro—components of an efficient molecular switch. Nature 294, 217–223. [PubMed: 6457992]

Ka D, An SY, Suh J-Y, and Bae E (2018). Crystal structure of an anti-CRISPR protein, AcrIIA1. Nucleic Acids Res. 46, 485–492. [PubMed: 29182776]

Lauer P, Chow MYN, Loessner MJ, Portnoy DA, and Calendar R (2002). Construction, Characterization, and Use of Two Listeria monocytogenes Site-Specific Phage Integration Vectors. J BACTERIOL 184, 11.

Loessner MJ (1991). Improved procedure for bacteriophage typing of Listeria strains and evaluation of new phages. Appl. Environ. Microbiol. 57, 882. [PubMed: 2039238]

Loessner MJ, Goeppl S, and Busse M (1991). Comparative inducibility of bacteriophage in naturally lysogenic and lysogenized strains of Listeria spp. by u.v. light and Mitomycin C. Lett. Appl. Microbiol. 12, 196–199.

Madar D, Dekel E, Bren A, and Alon U (2011). Negative auto-regulation increases the input dynamic-range of the arabinose system of Escherichia coli. BMC Syst. Biol. 5, 111. [PubMed: 21749723]

Meile S, Sarbach A, Du J, Schuppler M, Saez C, Loessner MJ, Kilcher S (2020). Engineered reporter phages for rapid bioluminescence-based detection and differentiation of viable Listeria cells. Appl Environ Microbiol. In press.

Mojica FJM, Díez-Villaseñor C, García-Martínez J, and Soria E (2005). Intervening Sequences of Regularly Spaced Prokaryotic Repeats Derive from Foreign Genetic Elements. J. Mol. Evol. 60, 174–182. [PubMed: 15791728]

Osuna BA, Karambelkar S, Mahendra C, Christie KA, Garcia B, Davidson AR, Kleinstiver BP, Kilcher S, and Bondy-Denomy J (2020a). Listeria phages induce Cas9 degradation to protect lysogenic genomes. co-submitted companion manuscript

Park SF, and Stewart GSAB (1990). High-efficiency transformation of Listeria monocytogenes by electroporation of penicillin-treated cells. Gene 94, 129–132. [PubMed: 2121618]

Rauch BJ, Silvis MR, Hultquist JF, Waters CS, McGregor MJ, Krogan NJ, and Bondy-Denomy J (2017). Inhibition of CRISPR-Cas9 with Bacteriophage Proteins. Cell 168, 150–158.e10. [PubMed: 28041849]

Rosenfeld N, Elowitz MB, and Alon U (2002). Negative Autoregulation Speeds the Response Times of Transcription Networks. J. Mol. Biol. 323, 785–793. [PubMed: 12417193]

Shimatake H, and Rosenberg M (1981). Purified λ regulatory protein c II positively activates promoters for lysogenic development. Nature 292, 128–132. [PubMed: 6264321]

Simon R, Priefer U, and Pühler A (1983). A Broad Host Range Mobilization System for In Vivo Genetic Engineering: Transposon Mutagenesis in Gram Negative Bacteria. Bio/Technology 1, 784–791.

Stanley SY, Borges AL, Chen K-H, Swaney DL, Krogan NJ, Bondy-Denomy J, and Davidson AR (2019). Anti-CRISPR-Associated Proteins Are Crucial Repressors of AntiCRISPR Transcription. Cell 178, 1452–1464.e13. [PubMed: 31474367]

Stern A, and Sorek R (2011). The phage-host arms race: Shaping the evolution of microbes. BioEssays 33, 43–51. [PubMed: 20979102]

Thieffry D, Huerta AM, Pérez-Rueda E, and Collado-Vides J (1998). From specific gene regulation to genomic networks: a global analysis of transcriptional regulation in Escherichia coli. BioEssays 20, 433–440. [PubMed: 9670816]

Trasanidou D, Gerós AS, Mohanraju P, Nieuwenweg AC, Nobrega FL, and Staals RHJ (2019). Keeping crispr in check: diverse mechanisms of phage-encoded anti-crisprs. FEMS Microbiol. Lett. 366, fnz098. [PubMed: 31077304]

Highlights

- Listeria anti-CRISPR protein AcrIIA1 serves as an anti-CRISPR and a vital autorepressor
- The rapid and strong *acr* promoter must be repressed for maximal phage fitness
- AcrIIA1 allows prophages to tune Acr expression to Cas9 levels
- AcrIIA1 homologs have been co-opted by the host as a “anti-anti-CRISPRs”

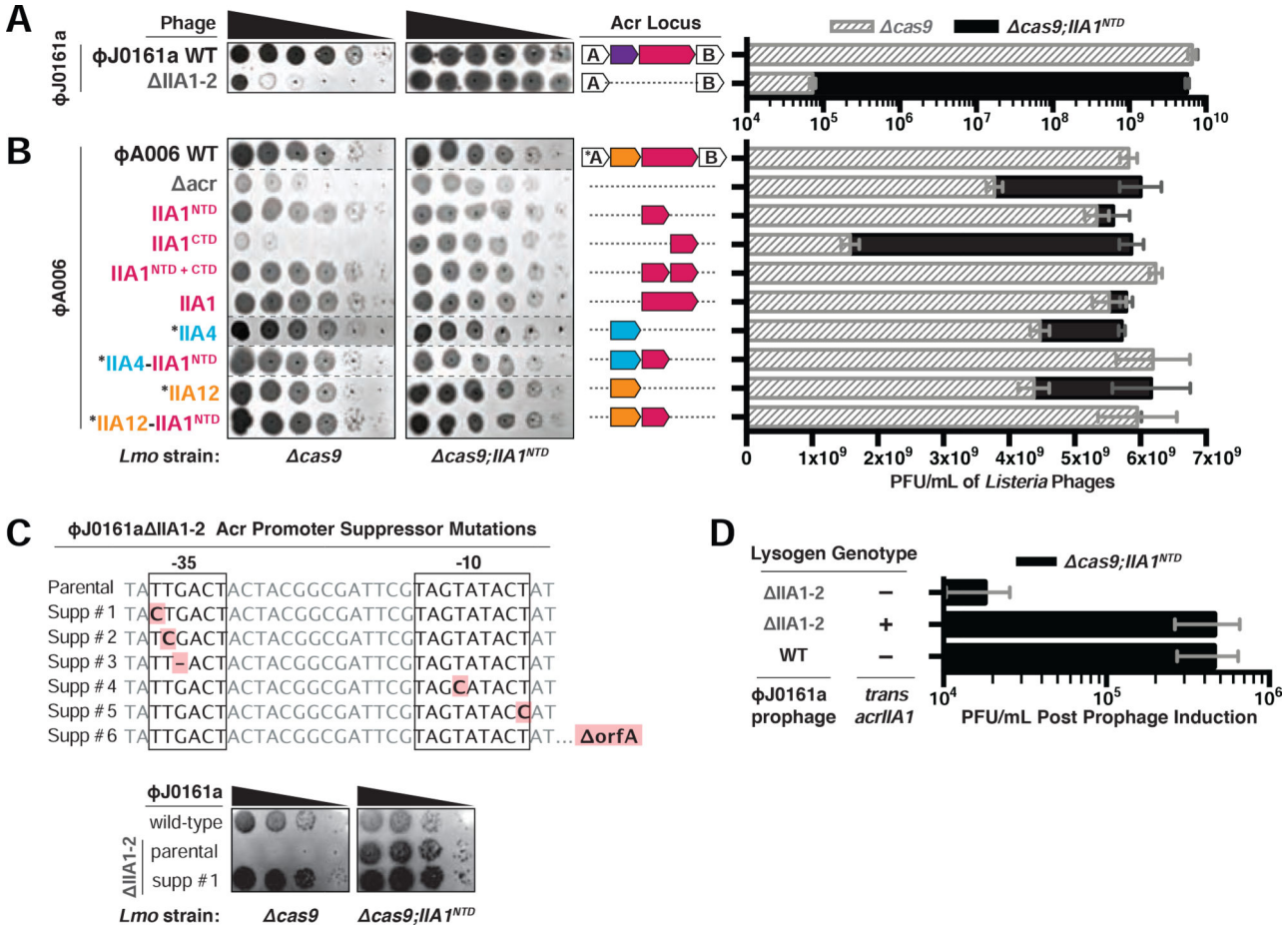

Figure 1. Phages Require the AcrIIA1^{NTD} (N-terminal Domain) for Optimal Replication

(A-B) Left: Representative images of plaquing assays where *Listeria* phages were titrated in ten-fold serial dilutions (black spots) on lawns of *Lmo*10403s (gray background) lacking Cas9 (*Δcas9*) and encoding AcrIIA1^{NTD} (*Δcas9;IIA1^{NTD}*). Dashed lines indicate where intervening rows were removed for clarity. Right: Cas9-independent replication of isogenic ΦJ0161a or ΦA006 phages containing distinct anti-CRISPRs. Asterisk (*) indicates genes that contain the strong RBS associated with orfA in WT ΦA006, whereas unmarked genes contain their native RBS. Plaque forming units (PFUs) were quantified on *Lmo*10403s lacking *cas9* (*Δcas9*, gray shaded bars) and expressing AcrIIA1^{NTD} (*Δcas9;IIA1^{NTD}*, black bars). Data are displayed as the mean PFU/mL of at least three biological replicates ± SD (error bars). See Figure S1A for phage titers of additional ΦA006 phages. (C) Top: Acr promoter mutations that suppress the ΦJ0161aΔIIA1–2 growth defect that manifests in the absence of *AcrIIA1^{NTD}*. Bottom: Representative images of suppressor (Supp) phage plaquing assays conducted as in A-B. (D) Induction efficiency of ΦJ0161 prophages. Prophages were induced with mitomycin C from *Lmo*10403s::ΦJ0161 lysogens expressing *cis-acrIIA1* from the prophage Acr locus (WT) or lacking *acrIIA1* (ΔIIA1–2) and *trans-acrIIA1* from the bacterial host genome (+) or not (−). Plaque forming units (PFUs) were quantified on *Lmo*10403s lacking *cas9* and expressing AcrIIA1^{NTD} (*Δcas9;IIA1^{NTD}*). Data are displayed as the mean PFU/mL after prophage induction of four biological replicates ± SD (error bars).

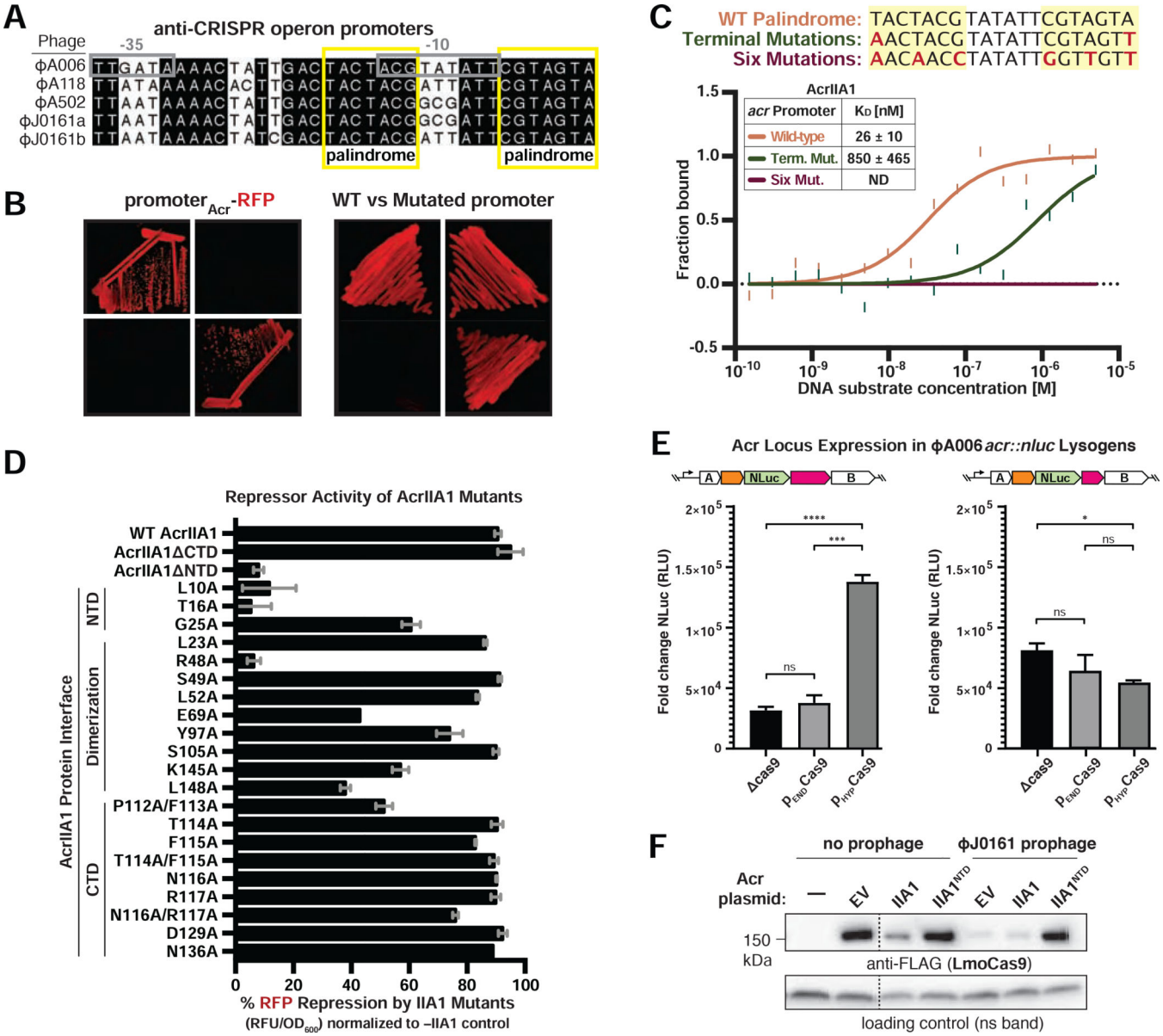

Figure 2. AcrIIA1^{NTD} autorepresses the *anti-CRISPR* locus promoter

(A) Alignment of the phage anti-CRISPR promoter nucleotide sequences denoting the −35 and −10 elements (gray boxes) and conserved palindromic sequence (yellow boxes). See Figure S2A for a complete alignment of the promoters. (B) Expression of RFP transcriptional reporters containing the wild-type (left) or mutated (right) ΦA006-$_{Acr.}$-promoter in the presence of AcrIIA1 (IIA1) or each domain (IIA1^{NTD} or IIA1^{CTD}). Representative images of three biological replicates are shown. (C) Quantification of the binding affinity (K_D; boxed inset) of AcrIIA1 for the palindromic sequence within the *acr* promoter using microscale thermophoresis. ND indicates no binding detected. The nucleotide mutations (red letters) introduced into each promoter substrate are listed above the graph. Data shown are representative of three independent experiments. (D) Repression of the ΦA006$_{Acr.}$−promoter RFP transcriptional reporter by AcrIIA1$_{ΦA006}$ mutant proteins.

Data are shown as the mean percentage RFP repression in the presence of the indicated AcrIIA1 variants relative to controls lacking AcrIIA1 of at least three biological replicates ± SD (error bars). (E) Nanoluciferase (NLuc) expression from the anti-CRISPR locus promoter in *Listeria* strains lysogenized with an ΦA006 reporter prophage (ΦA006*acr::nluc*) expressing AcrIIA1 (1) or AcrIIA1^{NTD} (1^{N}), in the presence of differing levels of Cas9: none (Δcas9), endogenous (P_{END}), overexpressed (P_{HYPER}). Data are shown as the mean fold change in RLU (relative luminescence units) of three biological replicates, i.e., independent lysogens ± SEM (error bars). p-values: ***<0.001, ****<0.0001 (F) Immunoblots detecting FLAG-tagged LmoCas9 protein and a non-specific (ns) protein loading control in *Lmo*10403s::ΦJ0161a lysogens or non-lyosgenic strains containing plasmids expressing AcrIIA1 (IIA1) or AcrIIA1^{NTD} (IIA1^{NTD}). Dashed lines indicate where intervening lanes were removed for clarity. Representative blots of at least three biological replicates are shown.

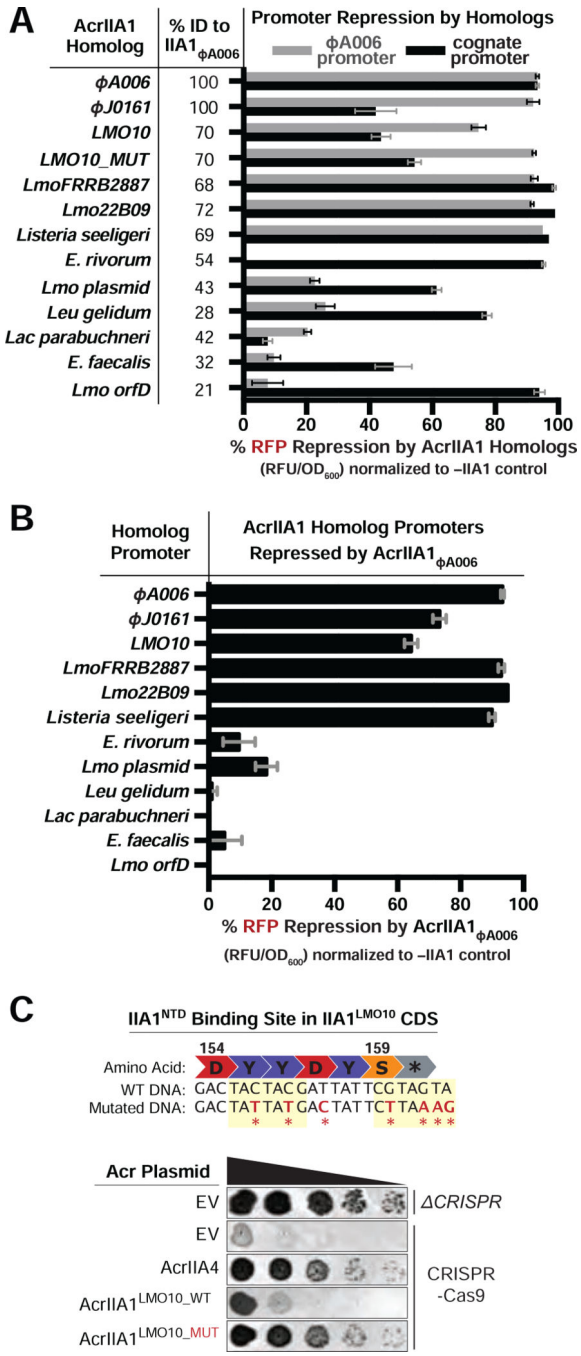

Figure 3. Autorepression is a General Feature of the AcrIIA1 Superfamily

(A-B) Repression of RFP transcriptional reporters containing the $\Phi A006_{Acr.}$–promoter (gray bars) or cognate-$AcrIIA1_{homolog}$.–promoters (black bars) by the indicated $AcrIIA1_{Homolog}$ proteins (A) or $AcrIIA1_{\Phi A006}$ protein (B). Data are shown as the mean percentage RFP repression in the presence of the indicated AcrIIA1 variants relative to controls lacking AcrIIA1 of at least three biological replicates ± SD (error bars). The percent protein sequence identities of each homolog to the $\Phi A006_{AcrIIA1}{}^{NTD}$ are listed in (A). (C) Top: Schematic of the wild-type (WT) and mutated $AcrIIA1^{NTD}$ binding site within the C-

terminal protein coding sequence (CDS) of AcrIIA1^{LMO10}. Bottom: Plaquing assays where the *P. aeruginosa* DMS3m-like phage JBD30 is titrated in ten-fold dilutions (black spots) on a lawn of *P. aeruginosa* (gray background) expressing the indicated anti-CRISPR proteins and Type II-A SpyCas9-sgRNA programmed to target phage DNA. Representative pictures of at least 3 biological replicates are shown.

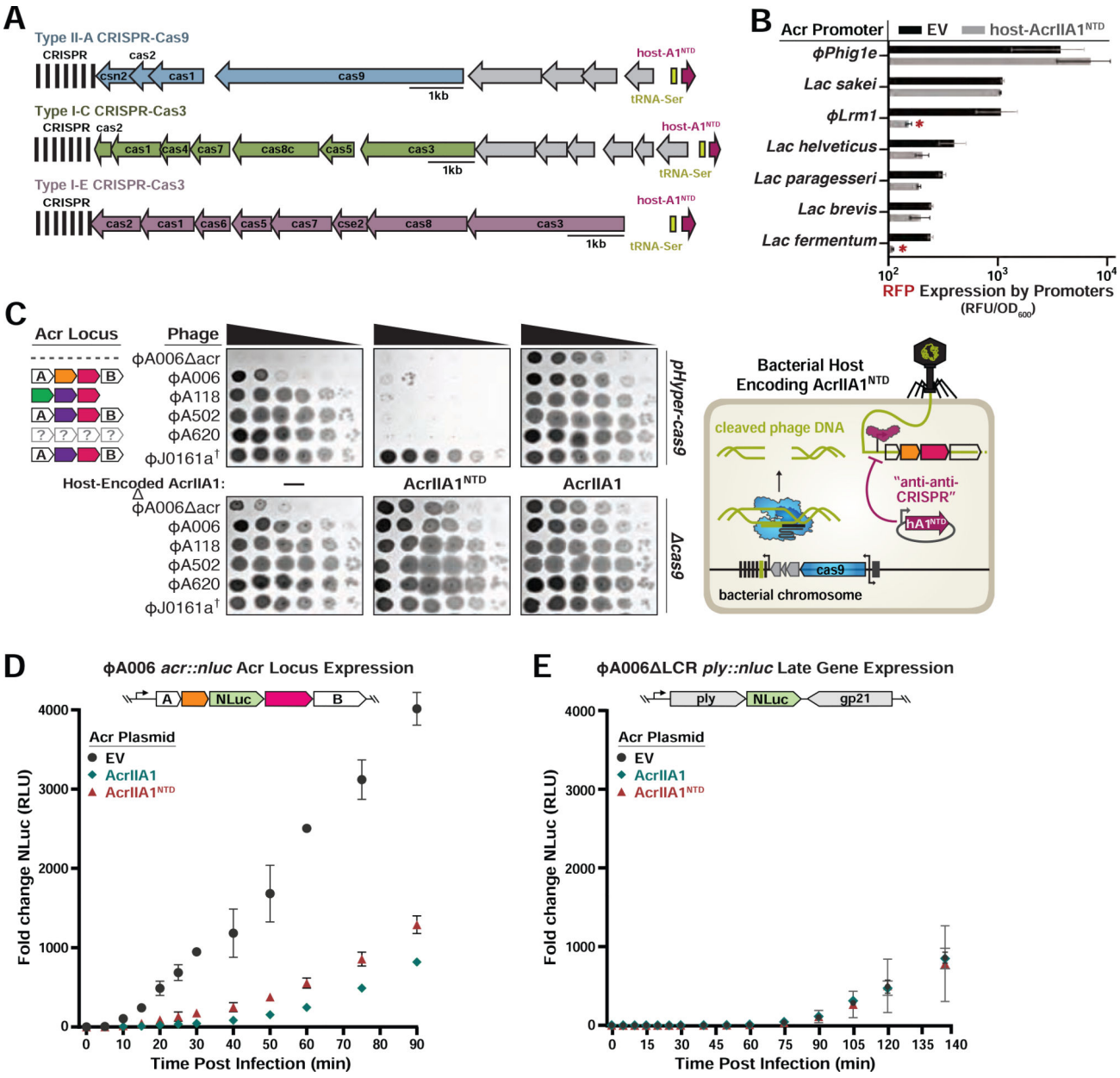

Figure 4. AcrIIA1^{NTD} Encoded from a Bacterial Host Displays "anti-anti-CRISPR" Activity

(A) Schematic of host-AcrIIA1^{NTD} homologs encoded in core bacterial genomes next to Type II-A, I-C, and I-E CRISPR-Cas loci in *Lactobacillus delbrueckii* strains. (B) Seven promoters from the indicated phages and prophages were placed upstream of RFP, in the presence or absence of host-encoded AcrIIA1^{NTD}, and fluorescence readout as in Figure 3. (C) Left panels: Plaquing assays where the indicated *L. monocytogenes* phages are titrated in ten-fold dilutions (black spots) on lawns of *L. monocytogenes* (gray background) expressing anti-CRISPRs from plasmids, LmoCas9 from a strong promoter (*pHyper-cas9*) or lacking Cas9 (Δ*cas)*, and the natural CRISPR array containing spacers with complete or partial matches to the DNA of each phage. (†) Denotes the absence of a spacer targeting the ΦJ0161a phage. Representative pictures of at least 3 biological replicates are shown. Right

panel: Schematic of bacterial “anti-anti-CRISPR” activity where host-encoded AcrIIA1^{NTD} (hA1^{NTD}) blocks the expression of anti-CRISPRs from an infecting phage. (D) Nanoluciferase (NLuc) expression from the anti-CRISPR locus promoter or a (E) late viral promoter during lytic infection (Meile et al., 2020). *L. monocytogenes* 10403S strains expressing AcrIIA1 or AcrIIA1^{NTD} from a plasmid were infected with reporter phages ΦA006*acr::nluc* or ΦA006 ΔLCR *ply::nluc*. Data are shown as the mean fold change in RLU (relative luminescence units) of three biological replicates ± SD (error bars).

KEY RESOURCES TABLE

REAGENT or RESOURCE	SOURCE	IDENTIFIER
Antibodies		
rabbit anti-FLAG	Sigma-Aldrich	Cat# F7425; RRID: AB_439687
mouse anti-FLAG	Sigma-Aldrich	Cat# F1804; RRID: AB_262044
HRP-conjugated goat anti-Rabbit IgG	Bio-Rad	Cat# 170-6515; RRID: AB_11125142
HRP-conjugated goat anti-mouse IgG	Santa Cruz Biotechnology	Cat# sc-2005; RRID: AB_631736
Bacterial and Virus Strains		
Listeria monocytogenes 10403s	Rauch et al., 2017	RefSeq: NC_017544.1
Listeria monocytogenes 10403s derivatives	This paper	See Table S2
Pseudomonas aeruginosa strain PAO1	Laboratory of Alan Davidson	RefSeq: NC_002516.2
Pseudomonas aeruginosa strain PAO1 derivatives	This paper	N/A
Escherichia coli DH5α	New England Biolabs	Cat #C2982I
Escherichia coli SM10	Laboratory of Daniel Portnoy	N/A
Listeria phage A006	This paper	RefSeq: NC_009815.1
Listeria phage A006 derivatives	This paper	See Table S2
Listeria phage A118	This paper	RefSeq: NC_003216.1
Listeria phage A502	This paper	RefSeq: MDRA00000000
Listeria phage A620	This paper	N/A
Listeria phage J0161a	Rauch et al., 2017	RefSeq: NC_017545.1
Listeria phage J0161a derivatives	This paper	N/A
Listeria phages P35	This paper	RefSeq: NC_009814.1
Pseudomonas phage JBD30	Laboratory of Alan Davidson	RefSeq: NC_020198.1
Chemicals, Peptides, and Recombinant Proteins		
AcrIIA1 protein homologs tested for promoter repression	This paper	See Table S1
Purified protein: AcrIIA1	This paper	N/A
Monolith His-Tag Labeling Kit RED-tris-NTA	Nanotemper Technologies	Cat #MO-L018
Tetrazolium Violet	TCI Chemicals	Cat #T0174
Critical Commercial Assays		
Gibson Assembly Master Mix	New England Biolabs	Cat #E2611 L
Phusion Hot Start Flex DNA Polymerase	New England Biolabs	Cat #M0535S
Oligonucleotides		
Listeria reporter phage lysogen confirmation Primer1: TAATTTGCTTAACTGATACC	This paper	N/A
Listeria reporter phage lysogen confirmation Primer2: TGACTACTACGTATATTCG	This paper	N/A
Wild-type Acr promoter for *in vitro* binding assay: AACTATTGACTACTACGTATATTCGTAGTATAATGTGAAT	This paper	N/A

REAGENT or RESOURCE	SOURCE	IDENTIFIER
Terminal Mutations Acr promoter for *in vitro* binding assay: AACTATTGACAACTACGTATATTCGTAGTTTAATGTGAAT	This paper	N/A
Six Mutations Acr promoter for *in vitro* binding assay: AACTATTGACAACAACCTATATTGGTTGTTTAATGTGAAT	This paper	N/A
Recombinant DNA		
AcrIIA1-associated promoter sequences	Twist Bioscience	See Table S1
pKSV7	Rauch et al., 2017	addgene.org/26686/
pKSV7-derivative plasmids	This paper	See Table S2
pPL2oexL	Rauch et al., 2017	https://doi.org/10.1016/j.cell.2016.12.009
pPL2oexL-derivative plasmids	This paper	See Table S2
pLEB579	Beasley et al., 2004	https://doi.org/10.1093/ps/83.1.45
pLEB579-derivative plasmids	This paper	See Table S2
pHERD30T	Laboratory of Alan Davidson	GenBank: EU603326.1
pHERD30T-derivative plasmids	This paper	N/A
pMMB67HE	ATCC	http://www.snapgene.com/resources/plasmid_files/basic_cloning_vectors/pMMB67HE/
pMMB67HE-derivative plasmids	This paper	N/A
pET28 protein expression plasmid	Laboratory of David Morgan	N/A
pET28-6xHis-AcrIIA1 protein expression plasmid	This paper	N/A
Software and Algorithms		
Prism 6.0	GraphPad	https://www.graphpad.com/scientific-software/prism/
Gen 5	BioTek	https://www.biotek.com/products/software-robotics-software/gen5-microplate-reader-and-imager-software/
Image Lab 5.2.1	BioRad	http://bio-rad.com/en-cn/product/image-lab-software
NanoTemper Analysis Software	NanoTemper Technologies	https://nanotempertech.com/monolith/
Other		
Synergy H1 Microplate Reader	BioTek	https://www.biotek.com/products/detection-hybrid-technology-multi-mode-microplate-readers/synergy-h1-hybrid-multi-mode-reader/
Azure c600 Imager	Azure Biosystems	https://www.azurebiosystems.com/imaging-systems/azure-600/
Monolith NT.115	NanoTemper Technologies	https://nanotempertech.com/monolith/